PHYSICAL REVIEW B VOLUME 11, NUMBER 12 15 JUNE 1975

Raman intensities in covalent crystals: A bond-polarizability approach*

Riccardo Tubino†
Department of Physics, New York University, New York, New York 10003

Luigi Piseri
Istituto di Chimica delle Macromolecole del CNR, Via A. Corti 12, 20133 Milano, Italy

(Received 20 November 1974)

A theoretical model for the calculation of the one- and two-phonon Raman scattering intensities (far from resonance) for covalent crystals is presented. Starting from Placzek's theory, the crystal polarizability is expressed as a sum of individual bond contributions. Instead of the usual "electron-phonon" and "electron-radiation" coupling constants, the Hamiltonian for the scattering process contains the bond polarizabilities and their derivatives with respect to the bond-stretching coordinates. The numerical value of such parameters has been obtained by Maradudin and Burstein from the experimentally known elasto-optic and electrostriction constants of the crystals. The two-phonon Raman spectrum of diamond is then calculated. The intensity trend is repoduced well and a number of interesting features are discussed. A new interpretation of the anomalous sharp line at the two-phonon cutoff is given.

I. INTRODUCTION

The development of laser Raman scattering provides a powerful tool for understanding the vibrational behavior of crystals. When dealing with single crystals the possibility of different scattering geometries is a source of different experimental information about phonon frequencies, selection rules, and Raman cross section.

While a number of reliable lattice-dynamical models have been developed in order to predict the position of the Raman peaks, less attention has been given to the interpretation of the Raman relative intensities. The aim of this paper is to discuss an electronic model suitable for the interpretation of the Raman cross section in covalent crystals for various scattering geometries. Actual calculations have been performed in this work on diamond crystal, whose second-order Raman spectrum contains a number of interesting and not completely explained experimental features.

The electronic model we are going to discuss is based on the so-called "bond-polarizability approximation" which has been clearly spelled out for the first time by Wolkenstein[1] and successfully applied to molecules.[2] Following Wolkenstein's assumptions, Long[3] developed a different mathematical treatment of the Raman intensity of molecules which is closely related to Wilson's G F technique[4] for normal vibrations.

Raman intensities in insulator crystals are usually[5] interpreted on the basis of quantities like electron-photon, electron-phonon, and electron-hole interactions, which correspond to a picture of the electronic structure of the crystal in terms of continuous band structure and energy gaps. As an alternate view we may regard a covalent crystal as a gigantic molecule with electrons distributed in closed shells, and along chemical bonds of a highly directional and localized character, as a consequence of the directional and localized nature of the atomic orbitals and their hybrids.[6] Along these lines it is possible to develop two consistent models for covalent crystals for the lattice dynamics and for the Raman cross sections in terms of forces producing deformations of lengths and bond angles and in terms of bond polarizabilities, following a development very close to the molecular case. Piseri *et al.*[7] developed the mathematical formulation needed to apply Wilson's GF technique to the study of the lattice dynamics of covalent crystals and actual calculations have been performed[8] for crystals of the group-IV elements (C, Si, Ge, and gray Sn). The main result of this calculation is that a surprisingly low number of "valence force constants" provides an excellent description of the phonon frequencies throughout the Brillouin zone, for all these crystals.

We will develop in this paper the algorithm for the calculation of the Raman relative intensities, in terms of the bond-polarizability theory. Also the results obtained for the diamond crystal will be reported.

II. PLACZEK THEORY AND RAMAN EFFECT IN CRYSTALS

The general expression for the Raman cross section can be derived using second-order perturbation theory. The intensity of a vibronic transition $(i \to f)$ when the incident light is polarized along the ρ direction and the scattered in the σ, is proportional to the square of the following quantity (neglecting damping)[9]

$$(\beta_{\rho\sigma})_{f\leftarrow i}=\frac{1}{\hbar}\sum_l\left(\frac{(P_{fl})_\rho(P_{li})_\sigma}{\omega_{lf}-\omega_f}+\frac{(P_{li})_\rho(P_{fl})_\sigma}{\omega_{li}+\omega_i}\right), \quad \rho,\sigma=x,y,z \tag{1}$$

where

$$(P_{kl})_\rho=\int\psi_k^*\left(\sum_i e_i\rho_i\right)\psi_l\,d\tau, \tag{2}$$

e_i being the charge localized at the point ρ_i so that $M_\rho=\sum_i e_i\rho_i$ represents the ρth component of the electric-dipole moment of the system. This formula is not very useful because the summation must be carried over all the excited vibronic states l of the system. The following assumptions are made to simplify this expression:

(i) The adiabatic approximation holds. A general vibronic state is then expressed in the following way:

$$\psi_{nv}(\xi x)=\phi_n(\xi x)\,u_{nv}(x) \tag{3}$$

(n and ξ refer to electronic, v and x to nuclear states).

(ii) The laser frequency ω is not close to any electronic excitations $\omega_{l\kappa}$ of the system and both are much larger than the vibrational frequencies.

(iii) The initial and the final states belong to the electronic ground states (vibrational Raman effect).

Provided that these conditions are fulfilled, Eq. (1) becomes

$$(\beta_{\rho\sigma})_{fi}\cong\int u_{0v_f}^*(x)\,\alpha_{\rho\sigma}(x)\,u_{0v_i}(x)\,dx=[\alpha_{\rho\sigma}]_{v_fv_i}. \tag{4}$$

The quantity $\alpha_{\rho\sigma}$ is known as the polarizability operator of the system and is given by

$$\alpha_{\rho\sigma}(x)=\frac{1}{\hbar}\sum_l\left(\frac{\Phi_{l\rho}(x)\,\Phi_{l\sigma}(x)}{\bar\omega_l-\omega_i}+\frac{\Phi_{l\rho}(x)\,\Phi_{l\sigma}(x)}{\bar\omega_l+\omega_f}\right), \tag{5}$$

where

$$\Phi_{l\rho}(x)=\int\phi_{n\,l}^*(\xi x)\,M_\rho\phi_0(\xi x)\,d\xi \tag{6}$$

and $\bar\omega_l$ means the vibronic frequency averaged on the all vibrational states belonging to a given excited state. This is the result of Placzek's theory[10] The scattering tensor for a transition between two nuclear states which belong to the same electronic state is equal to the matrix element of the polarizability tensor formed using the wave functions of the corresponding nuclear states. The limits of application of this theory are determined by the above stated assumptions (i)–(iii).

Formula (4) gives the expression for the scattered intensity in a more useful form since the polarizability of the system is now explicitly dependent on the nuclear coordinates and the nuclear wave functions $\vec{u}$ are known.

In the case of a crystal the total Raman-scattering intensity produced by incident light of electric field $\vec{E}$ scattered in the direction $\vec{s}$ is

$$I(\omega)=\sum_{\rho\sigma,\mu\nu}I_{\rho\sigma\mu\nu}(\omega)\,E_\rho E_\mu^*s_\sigma s_\nu, \tag{7}$$

where

$$I_{\rho\sigma\mu\nu}(\omega)=[\alpha_{\rho\sigma}]_{v_fv_i}[\alpha_{\mu\nu}^*]_{v_fv_i}. \tag{8}$$

The polarizability can be expanded in terms of the phonon normal coordinates of the crystal $\vec{Q}$,

$$\alpha_{\rho\sigma}=(\alpha_{\rho\sigma})_0+\sum_{\vec{q}j}\alpha_{\rho\sigma}(\vec{q},j)\,Q(\vec{q},j)+\sum_{\substack{\vec{q}_1\vec{q}_2\\ j_1j_2}}\alpha_{\rho\sigma}(\vec{q}_1,j_1;\vec{q}_2,j_2)\times Q(\vec{q}_1,j_1)\,Q(\vec{q}_2,j_2)+\cdots, \tag{9}$$

where j, j_1, and j_2 denote phonon branches.

By using Eqs. (9), (8), and (4) together with the expectation value of the phonon creation and destruction operators[11] one gets for the first- and second-order Stokes spectrum (recalling the momentum and energy conservation laws)

$$I^{\mathrm{I}}_{\rho\sigma\mu\nu}(\omega)=\sum_j\alpha_{\rho\sigma}(\vec{k},j)\,\alpha_{\mu\nu}(\vec{k},j)\times[n(\vec{k},j)+1]\,\delta(\omega-\omega(\vec{k},j)), \tag{10}$$

$$I^{\mathrm{II}}_{\rho\sigma\mu\nu}(\omega)=\sum_{\vec{q}j_1j_2}\alpha_{\rho\sigma}(\vec{q},j_1;-\vec{q},j_2)\,\alpha_{\mu\nu}^*(\vec{q},j_1;-\vec{q},j_2)\times[n(\vec{q},j_1)+n(\vec{q},j_2)+1]\times\delta(\omega-\omega(\vec{q},j_1)-\omega(\vec{q},j_2)), \tag{11}$$

where $\vec{k}\cong 0$ is the photon momentum and $\vec{q}$ is the phonon momentum. The theory outlined so far is general and can be used for evaluating the Raman-scattering intensity of any crystal, since no assumption has been made for the crystal polarizability derivatives with respect to normal coordinates. In order to perform an actual estimation of the $I_{\rho\sigma,\mu\nu}$ coefficients in Eqs. (10) and (11), the problem we are faced with is the calculation of the first and second derivatives of the crystal polarizability.

If the electrons of a crystal may be divided into a number of groups, which are supposed to be more or less independent of one another, the total wave function of the crystal (before being antisymmetrized) can be factored into a product of a set of functions describing the individual groups. The general quantum-mechanical expression for the crystal polarizability[12] will contain a term related to the statistical correlation between motions of electrons in two separate groups. This correlation will be zero if the groups of electrons are really independent. In this case it is easy to show that the total polarizability of the crystal is additive with respect to groups of electrons

$$\underline{\alpha} = \sum_n \underline{\alpha}_n , \tag{12}$$

where $\underline{\alpha}_n$ is the polarizability of the nth group of electrons. In the case of covalent crystals, electrons can be assumed to be localized in cores around single atoms and in chemical bonds. The crystal polarizability $\underline{\alpha}$ takes therefore the form

$$\underline{\alpha} = \sum_{j=1}^{N_B} \underline{\alpha}_j^B + \sum_{i=1}^{N_C} \underline{\alpha}_i^C , \tag{13}$$

where labels B and C refer to bonds and cores, respectively. The $\underline{\alpha}_j^B$ and $\underline{\alpha}_i^C$ are symmetrical 3×3 tensors. It is more convenient to refer the $\underline{\alpha}_j^B$ to the principal axis of the bond. For axially symmetric bonds (single and triple bonds) one gets

$$\overline{\underline{\alpha}}_j^B = \begin{pmatrix} \alpha_\perp^j & 0 & 0 \\ 0 & \alpha_\perp^j & 0 \\ 0 & 0 & \alpha_\parallel^j \end{pmatrix} ,$$
$$\overline{\underline{\alpha}}_i^C = \underline{\alpha}_i^C = \begin{pmatrix} \alpha_i & 0 & 0 \\ 0 & \alpha_i & 0 \\ 0 & 0 & \alpha_i \end{pmatrix} , \tag{14}$$

where $\overline{\alpha}$ tensors are expressed in the principal-axis system of each bond and $\perp$ and $\parallel$ refer to directions perpendicular and parallel to the bond, respectively. If $\underline{R}^j$ is the matrix which rotates the principal-axis system of the jth bond into crystal-fixed coordinates, one gets

$$\underline{\alpha}_j^B = \underline{R}_j^\dagger \overline{\underline{\alpha}}_j^B \underline{R}_j \tag{15}$$

and making use of the orthonormality relations for the direction cosines, one gets

$$(\underline{\alpha}_j^B)_{\rho\sigma} = (\alpha_\parallel^j - \alpha_\perp^j)(j\rho)(j\sigma) + \alpha_\perp^j \delta_{\rho\sigma} , \tag{16}$$

where $(j\rho)$ is the cosine of the angle between the jth bond and the ρth axis. The total polarizability of the crystal is thus given by

$$\alpha_{\rho\sigma} = \sum_{j=1}^{N_B} [(\alpha_\parallel^j - \alpha_\perp^j)(j\rho)(j\sigma) + \alpha_\perp^j \delta_{\rho\sigma}] + \sum_i^{N_C} \alpha_i , \tag{17}$$

N_B and N_C being the number of chemical bonds and atomic cores in the lattice, respectively.

It is apparent from Eq. (17) that a set of coordinates suitable for describing the crystal polarizability will contain the N_B bond stretchings and $3N_B$ changes in direction cosines, $2N_B$ of which are independent. This set of coordinates has been called intensity coordinates and is indicated by $\underline{I}_l$ (column vector containing the intensity coordinates belonging to the lth translational cell of the lattice). These coordinates are related to the Cartesian displacements (matrix $\underline{U}_l$) by a linear transformation

$$\underline{I}_l = \underline{T}_l \underline{U}_l . \tag{18}$$

For perfect lattices, phonon-displacement coordinates are used, by Fourier transforming the $\underline{U}_l$ matrices

$$\underline{U}(\vec{q}) = \sum_l \underline{U}_l e^{i\vec{r}(l)\cdot\vec{q}} , \tag{19}$$

where $\vec{q}$ is the phonon momentum and $\vec{r}(l)$ is the vector locating the lth cell in the direct lattice. We have then

$$\underline{I}(\vec{q}) = \underline{T}(\vec{q})\underline{U}(\vec{q}) , \tag{20}$$

where

$$\underline{T}(\vec{q}) = \sum_l \underline{T}_l e^{i\vec{r}(l)\cdot\vec{q}} . \tag{21}$$

(The elements of the $\underline{T}_l$ matrix are listed in Appendix A.) We have also that the phonon-normal coordinates are related to the phonon Cartesian displacements through the eigenvectors of the dynamical matrix:

$$\underline{Q}(\vec{q}) = \underline{L}^\dagger(\vec{q})\underline{U}(\vec{q}) . \tag{22}$$

Therefore, by arranging all the coordinates by columns, we get

$$\underline{I}(\vec{q}) = \underline{T}(\vec{q})\underline{L}(\vec{q})\underline{Q}(\vec{q}) , \tag{23}$$

$\underline{L}(\vec{q})$ being an orthogonal matrix. Using Eq. (23) it is possible to express now the derivatives of the crystal polarizability with respect to the normal coordinates in terms of more meaningful quantities

$$\alpha_{\rho\sigma}(\vec{q}, j) = \underline{\alpha}'_{\rho\sigma}\underline{T}(\vec{q})\underline{L}(\vec{q}, j) \tag{24}$$

and

$$\alpha_{\rho\sigma}(\vec{q}, j_1; -\vec{q}, j_2) = \underline{L}^\dagger(\vec{q}, j_1)\underline{T}^\dagger(\vec{q})\underline{\alpha}''_{\rho\sigma}\underline{T}(\vec{q})\underline{L}(\vec{q}, j_2) , \tag{25}$$

where $\underline{L}(\vec{q}, j)$ represents a column vector containing the eigenvector which describes the jth phonon branch, $\alpha'_{\rho\sigma}$ is a row whose general element $(\partial\alpha_{\rho\sigma}/\partial I_k)_{\text{equilibrium}}$ can be evaluated with the aid of Eq. (9), and $\underline{\alpha}''_{\rho\sigma}$ is a square matrix whose general element $(\partial^2\alpha_{\rho\sigma}/\partial I_k \partial I_l)_{\text{equilibrium}}$ can again be evaluated from Eq. (9).

For a covalent crystal a number of reasonable assumptions can be made in order to reduce the number of elements in $\underline{\alpha}'_{\rho\sigma}$ and $\underline{\alpha}''_{\rho\sigma}$.

First of all we notice that the core polarizability is clearly independent of the intensity coordinates and can therefore be neglected.

(i). The polarizability $\alpha_\perp^j$ and $\alpha_\parallel^j$ for each bond can be assumed to be dependent only upon the jth bond-stretching coordinate:

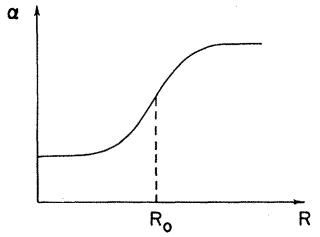

FIG. 1. Behavior of the bond polarizability as a function of the internuclear distance for a diatomic molecule.

$$\frac{\partial \alpha_{\parallel}^{j}}{\partial \vec{r}_k} = \frac{\partial \alpha_{\perp}^{j}}{\partial \vec{r}_k} = 0 \quad \text{for } j \neq k \tag{26}$$

(ii). The bond polarizability tensor can be assumed independent from the orientation of the bond,

$$\frac{\partial \alpha_{\parallel}^{j}}{\partial (k\rho)} = \frac{\partial \alpha_{\perp}^{j}}{\partial (k\rho)} = 0 \tag{27}$$

for each k and ρ.

(iii). A "typical" polarizability for a diatomic molecule, as a function of the internuclear distance is shown in Fig. 1. For $\vec{r}=0$ the bond polarizability is that of two atoms sticking together, while for $\vec{r}=\infty$ it is the sum of the individual atomic polarizabilities. Moreover, quantum-mechanical calculations for the H_2 molecule show[13] that $\underline{\alpha}$ is an essentially linear function of $\vec{r}$ in the vicinity of the equilibrium position, so that

$$\frac{\partial^2 \alpha_{\parallel}^{j}}{\partial \vec{r}^{\,2}} = \frac{\partial^2 \alpha_{\perp}^{j}}{\partial \vec{r}^{\,2}} = 0 . \tag{28}$$

By analogy with the molecular case[14] we will refer to the assumptions implied in Eqs. (26)–(28) as to the zero-order approximation. This is, of course, only an approximation since changes in angle configuration and stretching of the other bonds produce a rehybridization of the atomic orbitals which affect, to a certain extent, the polarizability of a given bond. In Appendix B the nonvanishing elements of α' and α'' in the zero-order approximation are reported. We notice that in order to calculate these derivatives the crystal polarizability must be expressed as a function of only $2N_B$ independent direction cosines.

We see therefore that within the zero-order approximation the intensity of the one-phonon and of the two-phonon spectrum should be dependent on the bond polarizabilities and their first derivatives, through coefficients determined by the crystal structure and by the forces acting in the lattice. The number of parameters is four times the number of "chemically different" bonds contained in each translational cell of the crystal. This situation is closely related to the lattice-dynamical model; and like the valence force constants the bond polarizabilities and their derivatives are not known *a priori*.

Depending on the complexity of the particular covalent crystal one is dealing with, different procedures could be used in order to perform a numerical evaluation of the parameters involved in our theory.

(a) If a reliable approximate wave function for the crystal can be worked out by the usual quantum-mechanical methods the polarizability can be approximated by a variational procedure suggested by Hylleraas[15] and Hasse.[16]

(b) Experimental measurements of the electric-field-induced infrared absorption have been reported for diamond[17] and for a number of other crystals. From the strength of this induced absorption the absolute value of the Raman-scattering tensor for the $\vec{q}=0$ optical modes can be evaluated and hence the bond polarizabilities [Eq. (10)]. A lattice-dynamical theory of the elasto-optic and electrostriction constants of crystals of the diamond structure has also been developed[18]: Bond polarizabilities and their derivatives are related to these experimentally determined constants.

(c) A set of bond polarizabilities values (and their derivatives) can be obtained by a least-squares fitting of the experimental intensities of the one- and two-phonon spectrum. This procedure is very close to that commonly used for obtaining the force constants from the experimental phonon frequencies. The intensity has to be expressed in a parametric form as a function of the electronic parameters, a Jacobian matrix has to be formed, and the usual least-squares-fitting procedure can be carried out.

We notice that, due to the quadratic form of Eq. (11), the dependence of the intensity on the parameters is not linear.

We are going to apply now the theory presented here to the case of diamond, for which bond polarizabilities and their derivatives have been obtained [case (b)].

III. APPLICATIONS TO DIAMOND

The Raman spectrum of diamond has been fully investigated by Solin and Ramdas[19] recently. It consists of a single one-phonon line at about 1333 cm^{-1} and a two-phonon scattering of much lower intensity with slope discontinuities and peaks. The spectrum has been recorded at three different temperatures and for different scattering geometries. One of the noteworthy features of the second-order spectrum is a sharp line at 2667 cm^{-1} (that is, at about the two-phonon cutoff) which is present in certain scattering geometries considered.

The position of the two-phonon peaks has been interpreted on the basis of the experimental coherent neutron-scattering data and of the joint

density of the states derived from different dynamical models.[8,20] The joint density of states derived from a shell model[20] and from a valence-force-field model[8] has sensibly the same structure and is reported in the lower half of Fig. 2. It shows a flat background up to 1500 cm^{-1} and a number of peaks, the most intense of which centered at about 1800 cm^{-1}. While the position of the kinks of the joint density of states agree with the position of the experimental peaks, the relative intensities are completely unrelated to the experimental situation. Moreover, the calculated density of states does not show any sharp peak corresponding to the 2667-cm^{-1} line observed experimentally.

Let us discuss now the results of the present calculations using the previously presented polarizability model. In the zero-order approximation four parameters are involved in the calculations, namely, $\alpha_{\parallel}$, $\alpha_{\perp}$, $\alpha'_{\parallel}$, $\alpha'_{\perp}$ of the C–C bond. In Table I are reported the values obtained by Maradudin *et al.*[18] for diamond which have been used in the present calculation. All the other parameters which determine the lattice dynamics of the diamond crystal (force constants, geometry) have been taken from Ref. 8.

Since diamond is a cubic crystal there are only three nonvanishing and independent components of the Raman tensor, namely, I_{XXXX}, I_{XXYY}, I_{XYXY} in terms of which the intensity of any scattering configuration can be expressed. The configurations given by Solin and Ramdas[19] refer to a system of axis related to the cubic axis as follows:

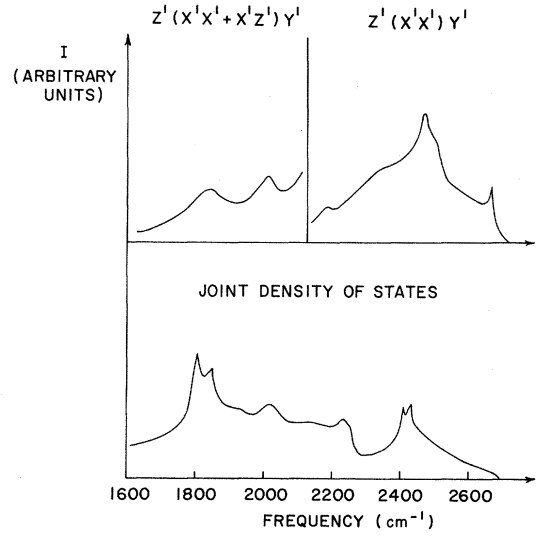

FIG. 2. Raman [$Z'(X'X'+X'Z')Y'$ and $Z'(X'X')Y'$ configurations] spectrum of diamond and two-phonon density of states. The intensity scale for the low-frequency section of the spectrum is enlarged with respect to the high-frequency part.

TABLE I. Parallel and perpendicular bond polarizabilities and their first derivatives for the diamond.

$\alpha_{\parallel}(\text{Å}^3) = 6.448$
$\alpha_{\perp}(\text{Å}^3) = -1.57$
$r_0\alpha'_{\parallel}(\text{Å}^3) = 9.62$
$r_0\alpha'_{\perp}(\text{Å}^3) = 1.17$

$$\begin{pmatrix} \vec{X}' \\ \vec{Y}' \\ \vec{Z}' \end{pmatrix} = \begin{pmatrix} 1/\sqrt{2} & 1/\sqrt{2} & 0 \\ 1/\sqrt{2} & -1/\sqrt{2} & 0 \\ 0 & 0 & 1 \end{pmatrix} \begin{pmatrix} \vec{X} \\ \vec{Y} \\ \vec{Z} \end{pmatrix}. \quad (29)$$

The components of the crystal polarizability in this new system are related to the ones referred to in the cubic axis by the transformation

$$\underline{\alpha}' = \underline{R}^{\dagger}\underline{\alpha}\underline{R}, \quad (30)$$

where $\underline{R}$ is the rotation matrix of Eq. (29).

In Table II Solin's scattering geometries are reported and expressed as a function of the three independent Raman-tensor components referred to the cubic axis.

In the case of diamond the polarizability tensor transforms as Γ_1^+, Γ_{12}^+, or Γ_{25}^+. The matrices corresponding to these three irreducible representations are given below:

$$\Gamma_1^+: \begin{vmatrix} a & 0 & 0 \\ 0 & a & 0 \\ 0 & 0 & a \end{vmatrix},$$

$$\Gamma_{12}^+: \begin{vmatrix} -b & 0 & 0 \\ 0 & -b & 0 \\ 0 & c & 2b \end{vmatrix}; \begin{vmatrix} b & 0 & 0 \\ 0 & -b & 0 \\ 0 & 0 & 0 \end{vmatrix},$$

$$\Gamma_{25}^+: \begin{vmatrix} 0 & d & 0 \\ d & 0 & 0 \\ 0 & 0 & 0 \end{vmatrix}; \begin{vmatrix} 0 & 0 & d \\ 0 & 0 & 0 \\ d & 0 & 0 \end{vmatrix}; \begin{vmatrix} 0 & 0 & 0 \\ 0 & 0 & d \\ 0 & d & 0 \end{vmatrix}.$$

Solin's scattering geometries can therefore pick up different components of the crystal polarizability. For example, for the $Y'X'$ configuration the intensity is proportional to $I_{XXXX} - I_{XXYY}$ which is $a^2 - a^2 = 0$ for the Γ_1^+ component, while it is $b^2 + b^2 = 2b^2$ for one of the Γ_{12}^+ components.

IV. COMPARISON WITH EXPERIMENT

We are now going to compare the experimental spectrum in the various scattering geometries with the calculated density of states and with the theoretical intensity predicted by our model. As a preliminary remark we notice that the force field

TABLE II. Scattering geometries for the diamond crystal.

$Z'(X'X')Y'$	$I \sim (\alpha_{X'X'})^2 = \frac{1}{2}I_{XXXX} + I_{XYXY} + \frac{1}{2}I_{XXYY}$	$\Gamma_1^+\Gamma_{12}^+\Gamma_{25}^+$
$Z'(X'Z')Y'$	$I \sim (\alpha_{X'Z'})^2 = I_{XYXY}$	Γ_{25}^+
$Z'(Y'X')Y'$	$I \sim (\alpha_{Y'X'})^2 = \frac{1}{2}(I_{XXXX} - I_{XXYY})$	Γ_{12}^+
$Y'(Z'Z')X'$	$I \sim (\alpha_{Z'Z'})^2 = I_{XXXX}$	$\Gamma_1^+\Gamma_{12}^+$

(on which the kink position depends) has been fitted[8] with respect to neutron coherent-scattering data[21] which have an experimental uncertainty up to 53 cm^{-1}, while optical measurements are much more accurate (see Table VII in Solin's paper) so we may expect possible shifts in the position of the kinks due to this reason.

In Fig. 2 the joint density of states (summation and overtones) is compared with the $(X'X')$ spectrum in the region 2050–2700 cm^{-1} and with the $(X'X'+X'Z')$ spectrum for the region down to 1600 cm^{-1}. The density of states shows a very strong kink at ~1800 cm^{-1}, while the experimental spectrum show a very weak peak at the corresponding frequency. The *strongest* feature of the experimental spectrum at ~2450 cm^{-1} corresponds to only a *medium*-intensity kink in the joint density. Finally, the density of states drops down to zero smoothly at the two-phonon cutoff.

In Figs. 3–6 the experimental spectrum in various scattering geometries is compared with the theoretical spectrum of Eq. (12).

The interaction Hamiltonian derived from the bond-polarizability theory using only four parameters turns out to be appropriate for describing the over-all intensity trend of the Raman scattering in diamond. As in the experimental spectrum for the region up to 2100 cm^{-1} the calculation shows

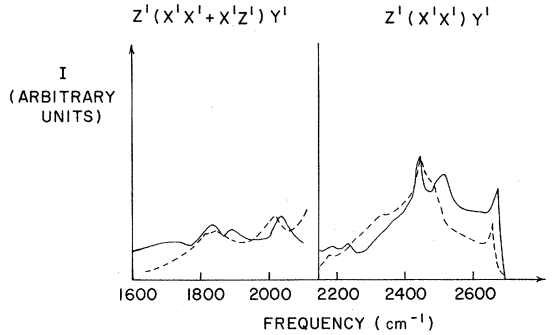

FIG. 3. Experimental (dashed line) and calculated Raman spectrum of diamond for $Z'(X'X'+X'Z')Y'$ and $Z'(X'X')Y'$ configurations. The intensity scale for the low-frequency section of the spectrum is enlarged with respect to the high-frequency part.

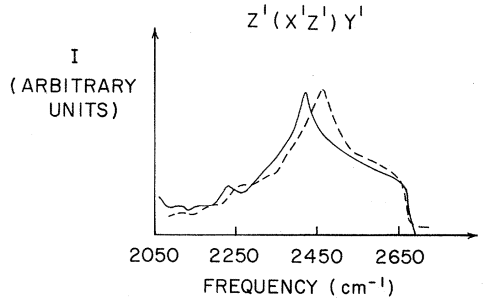

FIG. 4. Experimental (dashed line) and calculated Raman spectrum of diamond for $Z'(X'Z')Y'$ configuration.

a very weak quasicontinuous scattering [both in the experimental and in the calculated spectra two weak peaks can be observed with a more sensitive intensity scale (see Fig. 2)], while the most intense scattering is predicted for all the geometries in the region between 2400 and 2530 cm^{-1}. Moreover in the $(Z'Z')(Y'X')$ and $(X'X')$ configurations a sharp feature between 2660–2670 cm^{-1} is calculated, while this feature disappears in the $(X'Z')$ spectrum, in agreement with the experimental spectra. This sharp line has been variously interpreted. Cohen and Ruvalds[22] suggested that this line could be interpreted as a two-phonon resonance (bound state) whose energy lies above the two-phonon continuum. This bound state is generated by anharmonic interaction in the phonon Hamiltonian. The present calculation provides an alternative way of understanding the physical origin of this sharp line. Since no mechanical anharmonicity has been included in the phonon Hamiltonian this line can be viewed as due to a combination or an overtone, whose polarizability is particularly enhanced. In particular, we believe that the sharp line at 2667 cm^{-1} is due to the optical-phonon (Γ_{25}^+) overtone whose symmetry will be $(\Gamma_{25}^+)_2 = \Gamma_1^+ + \Gamma_{12}^+ + \Gamma_{25}^+$. This interpretation, supported by our results, is consistent with the experimental spectra, provided that, as calculations

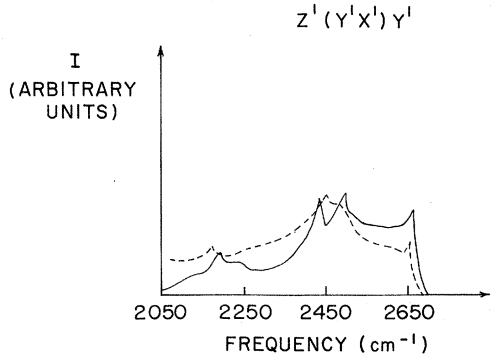

FIG. 5. Experimental (dashed line) and calculated Raman spectrum of diamond for $Z'(Y'X')Y'$ configuration.

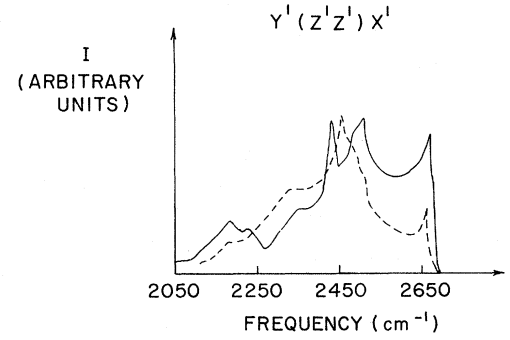

FIG. 6. Experimental (dashed line) and calculated Raman spectrum of diamond for $Y'(Z'Z')X'$ configuration.

show, the contribution from Γ_1^+ dominates the scattering process. The slight shift of 1.5 cm^{-1} above the two-phonon cutoff is accounted for by anharmonic corrections in the vibrational Hamiltonian.

On the basis of this calculation, the identification of the sharp peak slightly above the two-phonon cutoff with a two-phonon bound state becomes controversial. A detailed discussion of the subject goes beyond the original purpose of this paper, which is to provide a simple and general model for the calculation of the Raman-scattering intensities in covalent crystals. However, we are now using our model for studying this important point in more detail; and results will be reported more extensively elsewhere.

Another feature which is reproduced by the calculations is that in $(X'Z')$ configuration the 2450-cm^{-1} peak shows a very little fine structure, while all the other configurations show well-resolved additional peaks and shoulders.

In a few cases calculations and experiments are not in agreement.

(i) In the $(Y'X')$ configurations the 2050–2400-cm^{-1} range seems to have a rather high "plateau" of constant intensity, while calculations do not show this behavior.

(ii) The peak at 2180 cm^{-1} is usually broader in the calculated spectrum.

(iii) The main peak at 2450 cm^{-1} is usually followed by another twin peak at higher frequency in the calculations, while experiments show only a more or less pronounced shoulder of lower intensity

V. CONCLUDING REMARKS

We feel that the introduction of a polarizability-type Hamiltonian leads to a better understanding of the two-phonon Raman spectrum of diamond. The intensity trend can be considered satisfactory and the improvement compared to the joint density of states is considerable. Moreover, the proposed model provides a simple explanation for the sharp line at the two-phonon cutoff as due to a two-phonon scattering near to the zone center. The few discrepancies between calculations and experiments are easily understood as due to the simplicity of the model. It is likely that if the approximations implied in Eqs. (26)–(28) are removed and the number of parameters involved is increased, the fitting would be improved. Moreover, the experimental uncertainty on the electro-optic coefficients from which values for bond polarizabilities and their derivatives used in the present calculation have been derived, could play some role in modifying the shape of the computed spectra and to reduce the remaining discrepancies.

ACKNOWLEDGMENTS

One of the authors (R. T.) wishes to express his appreciation to Professor Joseph L. Birman for stimulating discussions and comments. This research was partially supported by the Italian National Research Council (C. N. R.) grant and by the National Science Foundation and also the Research Foundation of the City College of the CUNY.

APPENDIX A: EXPRESSION FOR T_l MATRIX ELEMENTS

a. Stretching coordinates. j and i are the atoms connected by the nth bond,

$$\frac{\partial R_n^{ij}}{\partial \beta_k} = (\delta_{kj} - \delta_{ki}) \cos(n\beta), \qquad \begin{matrix} \alpha, \beta = X, Y, Z; \\ k \text{ refers to atoms.} \end{matrix}$$

b. Changes in direction cosines.

$$\frac{\partial R_n \cos(n^{ij}\alpha)}{\partial \beta_k} = (\delta_{jk} - \delta_{ik})[\delta_{\alpha\beta} - \cos(n\alpha)\cos(n\beta)].$$

APPENDIX B: NON-VANISHING ELEMENTS IN α' USING THE N_B BOND STRETCHINGS AND $(nX), (nY)$ DIRECTION COSINES AS INTENSITY COORDINATES

$$\frac{\partial \alpha_{\rho\sigma}}{\partial r_n} = (\alpha'_{n\parallel} - \alpha'_{n\perp})(n\rho)(n\sigma) + \alpha'_{n\perp}\delta_{\rho\sigma} \quad \text{for } \rho, \sigma = X, Y, Z,$$

$$\frac{\partial \alpha_{\rho\sigma}}{\partial (n\rho)} = 2(\alpha_{n\parallel} - \alpha_{n\perp})(n\sigma) \quad \text{for } \rho, \sigma = X, Y,$$

$$\frac{\partial \alpha_{\rho z}}{\partial (n\sigma)} = -(\alpha_{n\parallel} - \alpha_{n\perp})\left(\frac{(n\rho)(n\sigma)}{(nz)}\right),$$

$$\frac{\partial \alpha_{\rho z}}{\partial (n\sigma)} = +(\alpha_{n\parallel} - \alpha_{n\perp})\left((nz) - \frac{(n\rho)^2}{(nz)}\right),$$

$$\frac{\partial \alpha_{zz}}{\partial (n\rho)} = -2(\alpha_{n\parallel} - \alpha_{n\perp})n\rho.$$

APPENDIX C: NONVANISHING ELEMENTS IN α''

$$\frac{\partial^2 \alpha_{\rho\sigma}}{\partial r_n^2} = (\alpha''_{n\parallel} - \alpha''_{n\perp})(n\rho)(n\sigma) + \alpha''_{n\perp}\delta_{\rho\sigma} \quad \text{for } \rho, \sigma = X, Y, Z,$$

$$\frac{\partial^2 \alpha_{\rho\sigma}}{\partial (n\rho)\,\partial (n\sigma)} = (1 + \delta_{\rho\sigma})(\alpha_{n\parallel} - \alpha_{n\perp}) \quad \text{for } \rho, \sigma = X, Y,$$

$$\frac{\partial^2 \alpha_{zz}}{\partial (n\rho)^2} = -2(\alpha_{n\parallel} - \alpha_{n\perp}),$$

$$\frac{\partial^2\alpha_{\rho z}}{\partial(n\sigma)^2} = -(\alpha_{n\parallel}-\alpha_{n\perp})\left(\frac{(n\rho)}{(nz)}+\frac{(n\sigma)^2(n\rho)}{(nz)^3}\right),$$

$$\frac{\partial^2\alpha_{\rho z}}{\partial(n\rho)^2} = -(\alpha_{n\parallel}-\alpha_{n\perp})\left(\frac{3(n\rho)}{(nz)}+\frac{(n\rho)^3}{(nz)^3}\right),$$

$$\frac{\partial^2\alpha_{\rho z}}{\partial(n\rho)\,\partial(n\sigma)} = -(\alpha_{n\parallel}-\alpha_{n\perp})\left(\frac{(n\sigma)}{(nz)}+\frac{(n\rho)^2(n\sigma)}{(nz)^3}\right),$$

$$\frac{\partial^2\alpha_{\rho\sigma}}{\partial r_n\,\partial(n\rho)} = (1+\delta_{\rho\sigma})(\alpha'_{n\parallel}-\alpha'_{n\perp})(n\sigma),$$

$$\frac{\partial^2\alpha_{\rho z}}{\partial r_n\,\partial(n\rho)} = (\alpha'_{n\parallel}-\alpha'_{n\perp})\left((nz)-\frac{(n\rho)^2}{(nz)}\right),$$

$$\frac{\partial^2\alpha_{\rho z}}{\partial r_n(n\sigma)} = -(\alpha'_{n\parallel}-\alpha'_{n\perp})\left(\frac{(n\rho)(n\sigma)}{(nz)}\right),$$

$$\frac{\partial^2\alpha_{zz}}{\partial r_n\,\partial(n\rho)} = -2(n\rho)(\alpha'_{n\parallel}-\alpha'_{n\perp}).$$

Note added in proof. After this work was submitted a paper on Raman scattering in diamond [S. Go, H. Bilz, and M. Cardona, Phys. Rev. Lett. 34, 580 (1975)] appeared. While details of the formalism used are not reported, the same approach, of expressing the crystal polarizability in terms of bond contributions, is adopted. The aim of our paper has been to check the validity of the bond polarizability theory by trying to predict the intensity of the spectra using parameters taken from independent experimental measurements. In their calculations, on the contrary, parameters have been obtained by fitting the experimental spectra. A number of their conclusions seem to be in agreement with the present results (in particular, the interpretation of the peak at the two-phonon cutoff). Their calculations, however, indicate that the approximation implied by Eq. (28) is not good for diamond.

---

†Present address: City College of the City University of New York, Physics Dept., New York, N.Y. 10031; Permanent address: Istituto di Chimica delle Macromolecole del CNR, Via A. Corti 12, 20133 Milano, Italy.

*Supported in part by the National Science Foundation Grant No. GH-31742.

[1]M. Wolkenstein, C.R. (Dokl.) Acad. Sci. SSSR 30, 791 (1941).

[2]M. Eliashevich and M. Wolkenstein, J. Phys. SSSR 9, 101, 326 (1945).

[3]D. A. Long, Proc. R. Soc. Lond. A 217, 203 (1953).

[4]E. B. Wilson, J. C. Decius, and P. C. Cross, *Molecular Vibrations* (McGraw-Hill, New York, 1955).

[5]J. L. Birman, *Handbuch der Physik* (Springer-Verlag, Berlin, 1974), Vol. 25/2b.

[6]C. A. Caulson, *Valence* (Clarendon, Oxford, 1952).

[7]L. Piseri and G. Zerbi, J. Mol. Spectrosc. 26, 254 (1968).

[8]R. Tubino, L. Piseri and G. Zerbi, J. Chem. Phys. 56, 1022 (1972).

[9]J. A. Koningstein, *Introduction to the Raman Effect* (Reidel, Dordrecht, 1972).

[10]G. Placzek, *Marx Handbuch der Radiologie*, 2nd ed. (Academische Verlagsgesellschaft, Leipzig, 1934), p. 209.

[11]R. A. Cowley, in *The Raman Effect*, edited by A. Anderson (Dekker, New York, 1971).

[12]J. O. Hirschfelder, *Molecular Theory of Gases and Liquids* (Wiley, New York, 1961).

[13]R. P. Bell and D. A. Long, Proc. R. Soc. Lond. A 203, 364 (1950).

[14]M. V. Wolkenstein, M. A. Eliashevich, and B. I. Stepanov, *Vibrations of Molecules* (State Publishers of Technical-Theoretical Literature, Moscow-Leningrad, 1949), Vol. 2.

[15]E. Hylleraas, Z. Phys. 65, 209 (1930).

[16]H. R. Hasse, Proc. Camb. Philos. Soc. 26, 542 (1930).

[17]E. Anastassakis and E. Burstein, Phys. Rev. B 2, 1953 (1970).

[18]A. A. Maradudin and E. Burstein, Phys. Rev. 164, 1081 (1967).

[19]S. A. Solin and A. K. Ramdas, Phys. Rev. B 1, 1687 (1970).

[20]G. Dolling and R. A. Cowley, Proc. Phys. Soc. Lond. 88, 463 (1966).

[21]J. L. Warren, J. L. Yarnell, G. Dolling, and R. A. Cowley, Phys. Rev. 158, 805 (1967).

[22]M. H. Cohen and J. Ruvalds, Phys. Rev. Lett. 23, 1378 (1969).